EPR Spectra of Mn^{2+}-Doped ZnS Quantum Dots

Pedro A. Gonzalez Beermann,[†] Bruce R. McGarvey,*[,‡]
Subra Muralidharan,*[,†] and Raymond C. W. Sung*[,†]

Department of Chemistry, Western Michigan University, Kalamazoo, Michigan 49008, and School of Physical Science, Chemistry and Biochemistry, University of Windsor, Windsor, Ontario, Canada N9B 3P4

Received June 17, 2003. Revised Manuscript Received October 3, 2003

Powder Mn^{2+} EPR spectra of 5-nm ZnS:Mn quantum dots have been analyzed in detail to account for all the observed fine spectral features. The same spectral features are observed in samples with low doping of Mn^{2+} (0.003−0.008%), showing 10 weak forbidden transitions between the six-line pattern of the $M_S = -1/2$ to $M_S = 1/2$ transition for the six M_I values. Spectral simulations have been performed with the Simfonia program with parameters $g_{xx} = 2.0064$, $g_{yy} = 2.0064$, $g_{zz} = 2.0066$, $D = 37.4 \times 10^{-4}$ cm^{-1}, $E = 12.5 \times 10^{-4}$ cm^{-1}, $A_{xx} = 63.9 \times 10^{-4}$ cm^{-1}, $A_{yy} = 64.0 \times 10^{-4}$ cm^{-1}, and $A_{zz} = 64.4 \times 10^{-4}$ cm^{-1}, suggesting a lower than T_d site symmetry for the doped Mn^{2+} in the cubic ZnS structure. At higher doping concentration (15.9%), a single broad line is observed with isotropic **g** and **A**.

Introduction

Electron paramagnetic resonance (EPR) has been widely used[1−6,14] to study Mn^{2+}-doped quantum dots, revealing structurally important information of the host lattice. The observed Mn^{2+} spectral features were used to explain the changes in the optical properties of the materials prepared by different methods. However, the spectral interpretations given were inadequate to account for all the observed fine structures, which may provide a better understanding of the system being studied.

In this paper we report the EPR study of ZnS:Mn with different amounts of Mn^{2+} doped into the lattice and provide a detailed explanation to account for all the observed fine spectral features. An in-depth characterization of the ZnS:Mn material including its luminescence, and interaction with molecules such as L-cysteine and L-methionine, will be published separately.[18] The use of Mn^{2+} EPR as a probe to study its surrounding lattice is well-known.[7,8] This is because Mn^{2+} has a total electronic spin $S = 5/2$, it is very sensitive to changes of its surrounding environment, and it monitors the crystal field directly via its spin Hamiltonian parameters. It has a long spin−lattice relaxation time, it can be easily doped into a host lattice, and its EPR spectrum is readily observable over a wide temperature range.

Experimental Section

Synthesis of Mn^{2+}-Doped ZnS (ZnS:Mn) Nanoparticles. A main objective of our research in this area of quantum dots is to investigate approaches for their synthesis in the aqueous medium from readily available precursors. A second objective of our program is the application of these quantum dots for the sensing of water-borne environmental pollutants. The ZnS:Mn nanoparticles were made by the following general procedure modified from that reported in the literature.[9] Ten milliliters of an aqueous solution of $Zn(CH_3COO)_2 \cdot 2H_2O$ (0.5 M) was added to 70 mL of $Na(PO_3)_n$ (10.2 g) with vigorous stirring at room temperature. Then 10 mL of $Mn(CH_3COO)_2 \cdot 4H_2O$ (0.2 M) was added in small portions to this solution. The mixture was sonicated to ensure complete dissolution. Next, 10 mL of Na_2S (0.5 M) was added at a flow rate of 0.7 mL/min using a peristaltic pump, and a white suspension was formed at this stage. The reaction temperature was maintained at ambient temperature for 2 h under constant stirring. The nanoparticles were isolated by centrifugation, washed twice with MilliQ water and then with cold ethanol (95% v/v), dried

* Corresponding authors. Tel., (519) 253-3000, ext. 3530; fax, (519) 973-7098; e-mail, beprm@uwindsor.ca (B. R. McGarvey). Tel., (269) 387-3656; fax, (269) 387-2909; e-mail, subra.murali@wmich.edu (S. Muralidharan). Tel., (269) 387-2077; fax, (269) 387-2909; e-mail, raymond.sung@wmich.edu (R. C. W. Sung).

[†] Western Michigan University.

[‡] University of Windsor.

(1) Hoffman, D. M.; Meyer, B. K.; Ekimov, A. I.; Merkulov, I. A.; Efros, Al. L.; Rosen, M.; Couino, G.; Gacoin, T.; Boilot, J. P. *Solid State Commun*. **2000**, *114*, 547.

(2) Igarashi, T.; Isobe, T.; Senna, M. *Phys. Rev. B* **1997**, *56*, 6444.

(3) Yu, I. L.; Isobe, T.; Senna, M. *J. Phys. Chem. Solids* **1996**, *57*, 373.

(4) Borse, P. H.; Srinivas, D.; Shinde, R. F.; Date, S. K.; Vogel, W.; Kulkarni, S. K. *Phys. Rev. B* **1999**, *60*, 8659.

(5) Dinsmore, A. D.; Hsu, D. S.; Qadri, S. B.; Cross, J. O.; Kennedy, T. A.; Gray, H. F.; Ratna, B. R. *J. Appl. Phys*. **2000**, *88*, 4985.

(6) Murase, N.; Jagannathan, R.; Kanematsu, Y.; Watanabe, M.; Kurita, A.; Hirata, K.; Yazawa, T.; Kushida, T. *J. Phys. Chem. B* **1999**, *103*, 754.

(7) Misra, S. K.; Sun, J. S. *Magn. Reson. Rev*. **1991**, *16*, 57.

(8) Upreti, G. C.; Chand, P. *Magn. Reson. Rev*. **1987**, *12*, 245.

(9) Bol, A. A.; Meijerink, A. *Phys. Rev. B* **1998**, *58*, R15 997.

(10) Bleaney, B. *Philos. Mag*. **1951**, *42*, 441.

(11) Walsh, W. M., Jr. *Phys. Rev*. **1961**, *122*, 762.

(12) Keller, S. P.; Gelles, I. L.; Smith, W. V. *Phys. Rev*. **1958**, *110*, 850.

(13) Abragam, A.; Bleaney, B. *Electron Paramagnetic Resonance of Transition Ions*; Clarendon Press: Oxford, 1970; p 440.

(14) Kennedy, T. A.; Glaser, E. R.; Klein, P. B.; Bhargava, R. N. *Phys. Rev. B* **1995**, *52*, R14 356.

(15) Qu, S. C.; Zhou, W. H.; Liu, F. Q.; Chen, N. F.; Wang, Z. G.; Pan, H. Y.; Yu, D. P. *Appl. Phys. Lett*. **2002**, *80*, 3605 .

(16) Levy, L.; Feltin, N.; Ingert, D.; Pileni, M. P. *Langmuir* **1999**, *15*, 3386.

(17) Cullity, B. D. *Elements of X-ray Diffraction*; Addison-Wesley Publishing Company, Inc.: Reading, MA, 1956; p 99.

(18) Gonzalez Beermann, P. A.; McGarvey, B. R.; Muralidharan, S.; Sung, R. C. W., to be submitted.

10.1021/cm030435w CCC: $27.50
Published on Web 02/13/2004

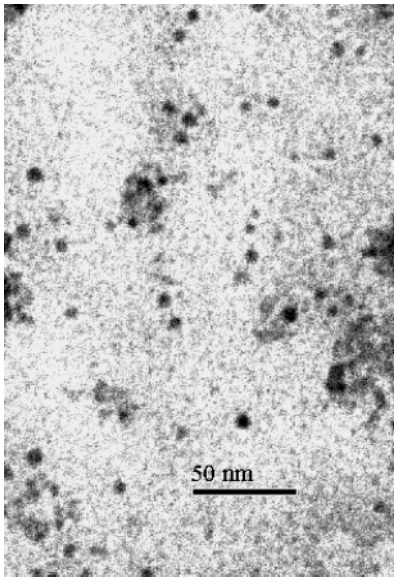

Figure 1. TEM micrograph of sample **3** at room temperature. The quantum dots have spherical shape with an average size of 5 ± 0.5 nm determined by counting a total of 30 particles from the micrograph.

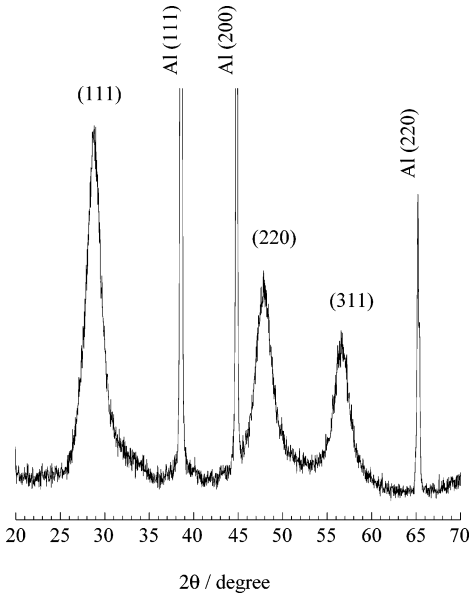

Figure 2. XRD diffractogram of sample **2** on an aluminum plate, acquired at room temperature using an XDS 2000 Scintac diffractometer. The pattern shows three broad peaks corresponding to the (111), (220), and (311) reflecting planes of the cubic ZnS structure.

under vacuum for 24 h, and ground in an agate mortar. Three ZnS:Mn powder samples were prepared in this way by varying the initial amount of Mn^{2+} salt used during the synthesis. The actual amount of Mn^{2+} doped into the ZnS lattice was determined by Chemisar Laboratories Inc., using a Varian Liberty 110 ICP. Then 50−100 mg of sample was accurately weighed and digested for 1 h in 5 mL of concentrated nitric acid. The digested sample solution was then cooled and diluted to a final volume of 25 mL using ultra-high-purity Millipore R.O. water prior to analysis using ICP-AES. Calibration was performed using NIST traceable standards for manganese. The results obtained were sample **1**, 0.003%, sample **2**, 0.008%, and sample **3**, 15.9%.

The morphology and size of the nanoparticles were determined using a JEOL JEM-1230 transmission electron microscope operated at an accelerating voltage of 80 kV. The average size of the quantum dots was determined to be 5 ± 0.5 nm, based on a total count of 30 particles from the TEM micrograph shown in Figure 1.

X-ray powder diffractions were performed using an XDS 2000 Scintac diffractometer. A diffractogram of sample **2** on an aluminum substrate, as shown in Figure 2, was obtained at room temperature, using Cu $K\alpha_1$ radiation with $\lambda = 0.15405$ nm. The XRD pattern showed the cubic structure of the host lattice. The average particle size was calculated using the Scherrer formula[17] to be 5.5 nm, in excellent agreement with that obtained from the TEM micrograph.

EPR Spectra. All EPR spectra were recorded at room temperature on an X-band Bruker ESP 300E spectrometer equipped with an electromagnet capable of providing a magnetic field range from 50 G to 15 kG, a microwave counter, and a gaussmeter. Typical measurement conditions were microwave power 20 mW, microwave frequency 9.7 GHz, modulation frequency 100 kHz, modulation amplitude 0.962 G, and 4k of data points covering a sweep width range from 450 to 5500 G. The powder samples used in the experimental measurements were sealed under vacuum in quartz tubes.

Spectral Analysis and Simulations

The powder spectra as shown in Figure 3a,b were obtained from samples **1** and **2** with 0.003 and 0.008% Mn^{2+} incorporated in ZnS. The spectrum is from the $M_S = -{}^1/_2$ to $M_S = {}^1/_2$ transition of Mn^{2+} in a nearly cubic site. To understand the spectrum, we must refer to the

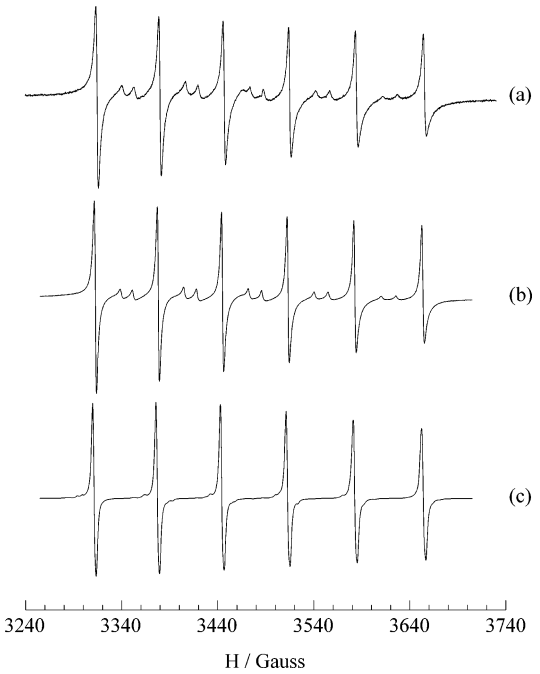

Figure 3. Room-temperature Mn^{2+} EPR spectra of ZnS:Mn powder specimens. (a) Experimental, 0.003% Mn^{2+}, (b) experimental, 0.008% Mn^{2+}, (c) simulation, 0.008% Mn^{2+} with parameters $g_{xx} = 2.0064$, $g_{yy} = 2.0064$, $g_{zz} = 2.0066$, $D = 37.4 \times 10^{-4}$ cm^{-1}, $E = 12.5 \times 10^{-4}$ cm^{-1}, $A_{xx} = 63.9 \times 10^{-4}$ cm^{-1}, $A_{yy} = 64.0 \times 10^{-4}$ cm^{-1}, and $A_{zz} = 64.4 \times 10^{-4}$ cm^{-1}.

spin Hamiltonian used to represent the spin states of the $S = {}^5/_2$, $I = {}^5/_2$ system of Mn^{2+}.

$$\hat{\mathcal{H}} = \beta_e \hat{\mathbf{S}}\cdot\mathbf{g}\cdot\mathbf{H} + D[\hat{S}_z^2 - {}^1/_3 S(S+1)] + E[\hat{S}_x^2 - \hat{S}_y^2] + \hat{\mathbf{S}}\cdot\mathbf{A}\cdot\hat{\mathbf{I}} - g_N\beta_N\hat{\mathbf{I}}\cdot\mathbf{H} + Q[\hat{I}_z^2 - {}^1/_3 I(I+1)] \quad (1)$$

The first term in the Hamiltonian is the electron Zeemann term, the second and third terms are the zero

Table 1. Spin Hamiltonian Parameters

host lattice	structure	**g** value	units of 10^{-4} cm^{-1}			reference
			$\|A\|$	$\|D\|$	$\|E\|$	
ZnS (samples **1** and **2**)	cubic[a]	$g_{xx} = 2.0064$	$A_{xx} = 63.9$	37.4	12.5	this work
		$g_{yy} = 2.0064$	$A_{yy} = 64.0$			
		$g_{zz} = 2.0066$	$A_{zz} = 64.4$			
ZnS (sample **3**)	cubic[a]	2.002	105			this work
zinc blende	cubic	2.0021	63.7			11
ZnS (Wurtzite)	hexagonal	2.0016	65	106		12
ZnS		2.0025	64			13
ZnS NC1		2.003	64.5			14
ZnS NC2		2.001	89	500−1000		
ZnS (A, B)		2.001	63.9	1		4
ZnS (C, D)		2.001	90.0			
ZnS (E)		2.0025	90.0			
ZnS, signal I	cubic	2.0024	64.5			2
ZnS, signal II	cubic	2.0013	84			

[a] Determined by XRD.

field spin−spin interaction, and the fourth term is the electron spin-nuclear spin interaction. The last two terms are the nuclear Zeemann and nuclear quadrupole terms that are much smaller and are often ignored, but cannot be ignored for this system. It should be noted that, for simplicity, we have left out an anisotropic term in the quadrupole interaction similar to the E term in the zero field interaction. The six main lines of the low Mn^{2+}-doped samples shown in Figure 3a,b are all that we could expect, if D and E were zero due to cubic site symmetry. The anisotropy in line width and shape of the six lines, however, tell us that the site symmetry is lower. Such asymmetry in the $M_S = -1/2$ to $M_S = 1/2$ spectrum can arise from anisotropy in any combination of anisotropy in the **g**, **A**, and zero field matrices. Attempts to duplicate this portion of the spectrum showed that we would have to assume anisotropy in all three matrices. A simulated spectrum obtained using the Bruker Simfonia program is shown in Figure 3c and the parameters used to obtain this simulation are summarized in Table 1, in comparison with those reported in the literature.[2,4,11−14] We found that any simulation that did not assume the magnitude of the parameter E to be close to the maximum value of $|D|/3$ produced additional lines from the $M_S = \pm 1/2$ to $M_S \pm 3/2$ or $M_S = \pm 3/2$ to $M_S \pm 5/2$ transitions that would be visible due to the narrow line widths needed to fit the observed lines. Also D cannot be much larger in magnitude than the value used to simulate Figure 3b.

The Simfonia program cannot simulate the ten peaks, between the main six lines, because they are forbidden transitions that were not included in the program. The six main lines are $M_S = -1/2$ to $M_S = 1/2$ transitions for the six values of M_I with M_I going from $5/2$ to $-5/2$ as magnetic field increases, if A is positive. The weaker lines, in between, are from double spin transitions where both M_S and M_I change simultaneously. The presence of the electronic zero field interaction and/or the nuclear quadrupole interaction causes a spin mixing of states, resulting in these transitions becoming weakly allowed. Going from low field to high field, the first forbidden transition to the right of the M_I main line is due to the M_I to $(M_I - 1)$ transition and the second to the $(M_I - 1)$ to M_I transition. If there were no nuclear Zeemann or nuclear quadrupole interactions, both of these transitions would occur halfway between the two main lines but a second-order nuclear spin-electron spin interaction term and the first-order nuclear Zeemann and quadrupole terms act to separate the two transitions. Using first- and second-order perturbation theory, the following equation has been derived[10] for the separation of the pair of lines observed between each pair of main lines.

$$\Delta = S(S+1)\frac{A^2}{H_0} + 2\left(\frac{g_N\beta_N}{g_e\beta_e}\right)H_0 - Q(3\cos^2\theta - 1)(2M_I - 1) \quad (2)$$

A and Q are in units of gauss, H_0 is the center magnetic field, and θ is the angle between the z-axis and the magnetic field. The above equation was obtained with the assumption that the electronic **g** matrix and the **A** matrix were isotropic. By definition, the five values of M_I in the above equation are $5/2$, $3/2$, $1/2$, $-1/2$, and $-3/2$.

The angular dependence of the quadrupolar term in eq 2 results in these "forbidden transitions" having an anisotropic powder spectrum, which is easily seen in both (a) and (b) of Figure 3. We should, however, obtain a good estimate of Δ by measuring the separation of the derivative peaks. In Figure 3b the values of Δ are 12.7, 13.2, 13.9, 14.5, and 15.3 G going from low to high field, giving an average of 13.9 G. According to eq 2, the quadrupole term drops out when we take the average, giving an average of

$$\Delta_{ave} = S(S+1)\frac{A^2}{H_0} + 2\left(\frac{g_N\beta_N}{g_e\beta_e}\right)H_0$$

This equation gives a value of 14.4 G for Δ_{ave}. This confirms our assignment of these peaks as electron−nuclear spin double spin transitions. The variation of the value of Δ tells us that there is a measurable quadrupole interaction but we cannot assign a value to Q because our assumption of axial symmetry in the quadrupole interaction is very likely wrong in this system. Including further anisotropy in the quadrupolar interaction will only introduce another unknown parameter to the equations. It should be emphasized that these extra transitions would not be visible if the site symmetry at the Mn^{2+} ion were truly cubic and are our strongest evidence that there is a small distortion from cubic at these sites.

Figure 4a shows the powder spectrum obtained from sample **3** with 15.9% Mn^{2+} content. The simulated

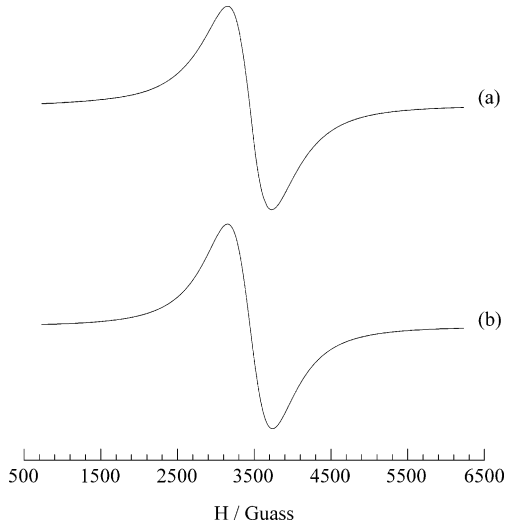

Figure 4. Room-temperature Mn^{2+} EPR spectra of ZnS:Mn powder specimen with 15.9% Mn^{2+} doping. (a) Experimental and (b) simulation with parameters $g = 2.002$ and $A = 105 \times 10^{-4}$ cm^{-1}.

spectrum as shown in Figure 4b assumes an isotropic **g** and **A** with magnitudes given in Table 1.

Results and Discussion

The quantum dots, as shown by the TEM micrograph in Figure 1, have spherical shape with an average size of 5 ± 0.5 nm, which is in agreement with the value calculated from the XRD data. The slight aggregation is due to the melting of some of the nanoparticles over a prolonged exposure of the sample to the electron beam. The result from the X-ray diffractogram, as shown in Figure 2, shows three broad peaks corresponding to the (111), (220), and (311) reflecting planes of the cubic ZnS structure as reported elsewhere.[6,15] There is also no change in the position of the peaks for both the doped and undoped ZnS. The three sharp peaks, as labeled Al(111), Al(200), and Al(220) on the figure, arise from the diffractions of the substrate aluminum.

The EPR results as summarized in Table 1 provide a direct comparison of the spin Hamiltonian parameters obtained from this study and those reported in the literatures.[2,4,11−14]

Our powder samples with very low Mn^{2+} content have an average A value of about 64×10^{-4} cm^{-1}, which is in agreement with all the reported literature values for internally Mn^{2+}-doped ZnS. The small anisotropy of the six hyperfine lines indicates that there is a small distortion of the T_d site symmetry in the cubic ZnS structure, at least for the doping sites. This is further supported by the small D and E values. Since the ionic radius of Mn^{2+} ion is about 10% larger than that of Zn^{2+}, the substitution has forced a small change of the site symmetry. The fact that there is no noticeable change in the XRD pattern suggests that EPR is a more sensitive and revealing technique to probe the changes in a crystal lattice structure. The "forbidden transitions" between the six main hyperfine lines have been observed in similar systems in the past; their appearances are either ignored or only very briefly mentioned[4,16] without much effort to explain their occurrence. This is, to the best of our knowledge, the first time that a detailed analysis of such kind of spectral feature is given for the system. We believe that these transitions are size-independent because they are also seen in systems[1−4,16] with different particle sizes at low Mn^{2+} concentration. The disappearance of these transitions at higher Mn^{2+} concentration is apparently due to the masking of a different Mn^{2+} spectrum, which has a very different set of spin Hamiltonian parameters.

At higher Mn^{2+} concentration a single broad line is observed with isotropic g and A values given in Table 1. The broad line feature is the result of Mn^{2+}−Mn^{2+} interactions due to their close proximity. The spectrum has an A value of about 105×10^{-4} cm^{-1}, which is significantly greater than all the reported literature values[2,4,14] for surface doping. As a purely speculative guess, there may be some cluster formation within the ZnS lattice at such a high Mn^{2+} concentration. We hope to see a change in the spectral features at some intermediate Mn^{2+} concentration, which may provide further information to resolve the uncertainty. We are unable to achieve this with the samples used in this study.

Conclusions

A detailed interpretation of the EPR spectra of ZnS:Mn powders with low Mn^{2+} concentration has been given, and the spin Hamiltonian parameters indicate that Mn^{2+} has a lower than T_d site symmetry in the cubic ZnS structure. The broad line spectral feature at higher Mn^{2+} concentration is due to Mn^{2+}−Mn^{2+} dipolar interactions, possibly due to some cluster formation in the lattice.

Acknowledgment. This research was supported by the Michigan Life Science Corridor (MLSC). Pedro A. Gonzalez Beermann acknowledges support from the Laspau and Fullbright Exchange Program for his doctoral studies at Western Michigan University.

CM030435W